

Phytoplankton were dominated by species of *Chryso-sphaerella*, *Dinobryon*, and *Tabellaria* throughout the 20-year period. These genera are typical of natural lakes in the area [(8); H. J. Kling and S. K. Holmgren, *Can. Fish. Mar. Serv. Tech. Rep.* 337 (1972)].

21. The effects of nutrients, light, and temperature on phytoplankton are discussed in D. W. Schindler, *Limnol. Oceanogr.* **23**, 478 (1978).
22. Phytoplankton production was measured with ^{14}C [J. A. Shearer, E. R. DeBruyn, D. R. Declercq, D. W. Schindler, E. J. Fee, *Can. Fish. Aquat. Sci. Tech. Rep.* 1341 (1985)]. The photosynthesis per unit light at submaximal rates and the rate of maximum photosynthesis varied synchronously in lakes of the area spanning several orders of magnitude in size. The total magnitude of variation was a factor of 2 to 3 in all cases. These results suggest that the responses of phytoplankton production in small lakes like Lake 239 can be extrapolated to lakes of all sizes in the same region (E. J. Fee and R. E. Hecky, unpublished data). However, as in the ELA lakes, the variations in phytoplankton production in larger lakes showed no significant correlation with climatic variables.
23. The distribution of filamentous green algae in the shallows of Lake 239 has been mapped annually during the late summer (M. Jackson, personal communication). During 1982 to 1987, epiphytic coverage by filamentous green algae (chiefly of the genus *Mougeotia*) has been proportional to epilimnetic temperature. The species changes resemble those seen during early acidification of Lake 302S [M. A. Turner *et al.*, *Can. J. Fish. Aquat. Sci.* **44** (suppl. 1), 135 (1987)]. Increasing concentrations of atmospheric CO_2 are also expected to cause a slight increase in the photosynthesis of epiphytic algae in softwater lakes (M. A. Turner, unpublished data). No stimulation of phytoplankton photosynthesis due to increased CO_2 is expected [J. A. Shearer and E. R. DeBruyn, *Water Air Soil Pollut.* **30**, 695 (1986); E. R. DeBruyn, unpublished data]. From 1981 to 1988, maximum annual rates of photosynthesis by epilithiphyton in Lake 239 were also related to maximum epilimnion temperature (M. A. Turner, unpublished data). Contrary to our initial expectations, epilithic respiration was unaffected by epilimnion temperature.
24. Organisms that may be adversely affected by increasing temperature include the lake trout *Salvelinus namaycush* and the opossum shrimp *Mysis relicta*. Both are important in the food chains of boreal lakes with oxygen-rich conditions and temperatures less than 16°C . Both species are also very susceptible to lake acidification, which is also occurring in many boreal lakes (25). Prolonged summer stratification also prolongs the period during which oxygen depletion in hypolimnions can occur [P. V. Eloranta, *Water Res.* **17**, 133 (1983)].
25. D. W. Schindler *et al.*, *Science* **228**, 1395 (1985).
26. Geographical distribution maps of fishes in lakes that are suitable are given by W. B. Scott and E. J. Crossman [*Fish. Res. Board. Can. Bull.* **184**, 1 (1973)]; M. J. Dadswell [*Zool. II* (Nat. Mus. Nat. Hist., Ottawa, 1974)] gives similar information for relict glacial crustaceans.
27. An example of how the disappearance of key food organisms can disrupt fish production in boreal lakes is given in (25).
28. This work was supported by the Canadian Department of Fisheries and Oceans. P. Campbell, I. J. Davies, R. E. Hecky, G. Koshinsky, and H. E. Welch reviewed the manuscript. B. Parker assisted with data analysis.

10 August 1990; accepted 20 August 1990

Ridge Spreading, Subduction, and Sea Level Fluctuations

MICHAEL GURNIS

A numerical model of mantle convection shows that sea level fluctuations are not simply associated with temporal changes in oceanic plate spreading. In the dynamic model, sea level rises rapidly and then falls toward a steady value (but one still higher than the initial) following increased ridge spreading; this time dependence results from profound changes in the deep thermal structure under ocean and continent. The use of past variations in oceanic spreading to infer sea level fluctuations is called into question. With more realistic models and better continental stratigraphy, constraints may be placed on the viscosity structure of the mantle.

WITHIN A FEW YEARS AFTER THE acceptance of plate tectonics, Hays and Pitman (1) among others, pointed out that the well-documented Cretaceous transgression occurred at approximately the same time as an increase in the spreading of oceanic plates. Since then, the prevailing view has been that increased rates of plate spreading give rise to an increased volume of oceanic ridges and a decreased volume of ocean basins (2). For a constant volume of water, continental platforms have been thought to flood during

periods of increased spreading. The determination of past variations in spreading has thus been viewed as an alternative method to estimate global eustatic sea level variations (3). This lithospheric model fails to conserve mass, however, because the cold oceanic lithosphere subducting into the mantle is ignored and implicitly assumed to disappear. With a simple model of mantle convection, I show that changes in plate velocity lead to changes in the rate at which cold lithosphere returns to the mantle and that this process leads to sea level fluctuations fundamentally different in both form and magnitude from the lithospheric model. Earlier, Hager (4) pointed out some dynamic problems encountered in relating oceanic

spreading rates directly to changes in sea level and he suggested that sea level could either rise or fall with increased spreading, depending on whether slabs are returned to the mantle under continents or under oceans, respectively.

Failure to conserve mass is overcome with the use of a simple thermal-convection calculation in which the oceanic lithosphere acts as an integral part of the overall system of heat and mass transfer. In a two-dimensional rectangular region, the equations of motion, continuity, and energy are solved simultaneously for an infinite Prandtl number and incompressible fluid; a finite-element formulation (5) is used to solve these equations. The technique used for simulating oceanic plates is similar to the one presented by Davies (6), except that a more stringent set of boundary conditions is used in which the entire oceanic lithosphere moves with horizontally uniform velocity. The use of a kinematically imposed lithosphere provides a framework in which to set up well-posed sea level experiments. Sea level variations caused by variable plate velocity can be directly assessed with this model, and thus the more circuitous method of a fully dynamic model (7) can be avoided. In order to control plate velocity with a fully dynamic model, the heat added to the system or a material property must vary; at this exploratory stage, such a complex technique (although a potentially more powerful one) is unwarranted.

The two-dimensional model [(8), Fig. 1, A to C] includes both an oceanic region, extending from $x = 0$ to $x = X_c$, and a continental region, extending from $x = X_c$ to $x = X_1$. The shaded areas in Fig. 1B denote zones of uniformly imposed velocity. With a box depth of D , the models had $X_c/D = 3$ and $X_1/D = 5$; these values were chosen so that the ratio of continental area to total surface area is 0.4. At both $x = 0$ and $x = X_1$, the side boundaries are reflecting. Because the oceanic plate has a uniform positive velocity, a symmetrical spreading ridge forms at the origin, and the lithosphere explicitly subducts at $x = X_c$; the continental plate has zero velocity. For this system with a constant viscosity throughout, sea level variations are computed in the following way. On the top surface of the convecting fluid, the topography (called the dynamic topography, w_d) is determined from the vertical deviatoric stress and explicitly includes the contributions from the subsiding oceanic lithosphere. An isostatic component to the topography, w_c , implicitly caused by crustal thickness variations, is added to the area over the continental lithosphere. In other studies involving the interaction of conti-

Department of Geological Sciences, University of Michigan, Ann Arbor, MI 48109.

nents with dynamic topography (9), w_c was assumed to be represented by the average topography of the continents, w'_c . It would be much more realistic if both dynamic topography and continental isostatic topography were summed to the observed shape of the continents. This is impractical because, as shown below, w_d is a strong function of time. Instead, we assume that

$$w_c = w'_c - w_d(0) \quad (1)$$

where $w_d(0)$ is the initial dynamic topography (that is before a plate rearrangement has occurred); w'_c is taken to be the observed continental hypsometry for all continents (10); the maximum change in isostatic topography is h_c . The last contribution to the topography results from a constant volume of ocean water, w_w . Water is locally compensated and added to the system, starting from the topographically lowest point, such that each mass column is in isostatic equilibrium with respect to w_d . The water surface should follow the geoid, but in constant-viscosity systems (such as the one studied here) the admittance, or ratio of geoid to dynamic topography, does not exceed about 0.11; when the admittance is as small as this, sea level variations are dominated by variations in dynamic topog-

raphy (9). In summary, the total topography is

$$w_T = w_d - w_d(0) + w'_c + w_w \quad \text{for } x > X_c$$

$$w_T = w_d + w_w \quad \text{for } x < X_c \quad (2)$$

Thus, w_d is the driving term in the topography caused by convection, and w_w responds to those changes. Sea level is defined as the difference between the average height of the continental surface (including the flooded portions) and the average height of the water surface.

A scheme for normalizing the topographic height (including sea level) and time was chosen such that the dynamic cause of sea level fluctuations will be readily apparent. In the numerical experiments, plate velocity was suddenly changed at a time zero and normalized by $\tau = X_c/V_2$, where V_2 is the new plate velocity and τ is the time for the oceanic lithosphere to reach a new steady-state structure. All sea level fluctuation predicted by the lithosphere model occurs within τ . Topographic heights were normalized by h_c so that fluctuations in dynamic relative to isostatic topography will be readily apparent.

The sea level variations resulting from the convection model will be compared to the standard model in which topography in the

oceanic region is obtained from boundary layer theory. In this model, the topography over the lithosphere, w_L , decreases (with respect to the ridge crest) as (2)

$$w_L = -2\alpha(T_m - T_o)(\kappa t/\pi)^{1/2} \quad (3)$$

where α is the coefficient of thermal expansion, T_m is the temperature of the mantle, T_o is the temperature on the sea floor, κ is the thermal diffusivity, and t is the age of the lithosphere. By setting $w_d = w_L$ for $x < X_c$ and $w_d = 0$ for $x > X_c$ in Eq. 2, the same procedure followed for computing sea level in the convection model can also be followed for the lithosphere subsidence model. The results (11) (Fig. 2, curve *a* for the case where plate velocity is increased by three-halves and curve *b* for the case where plate velocity is decreased by two-thirds) show that sea level in the standard model undergoes an initial rapid rise with a slow convergence to a new (higher) steady-state value when spreading rate increases. When spreading rate drops, sea level falls. As expected, the time scale for the readjustment in sea level is unity for both cases (Fig. 2).

The dynamic-convection model shows fundamental differences from the lithosphere model (Fig. 2). When the spreading rate is again increased to three-halves of its earlier value (curve *d*), sea level increases faster than predicted by the lithosphere model. But more fundamentally, at about time 0.7, sea level starts to fall and comes to a steady state in about 2.5 time units. The steady-state value is only 54% of the value predicted by lithospheric subsidence alone, and it is only 50% of the maximum in sea level, which occurred at time 0.7. The behavior of the model in which spreading rate decreases to two-thirds of its earlier value shows much the same behavior: a strong initial overshoot in sea level followed by a steady-state sea level change smaller than predicted by the lithospheric model alone. The steady-state value is only 40% of the maximum change in sea level, which occurred at about time 0.6. This complicated time dependence results from changes in the thermal state under both continent and ocean.

These deviations from the simple lithosphere-subsidence model are easily understood in the context of the time dependence of the differential temperature for the model in which plate velocity increases (Fig. 1, D and E). As the plate thins, the top part of model representing the oceanic lithosphere becomes hotter, as predicted from boundary layer theory. Considered alone, this change in temperature would lead to sea level fluctuations approximated by curve *a* in Fig. 2. But the faster oceanic plate velocity

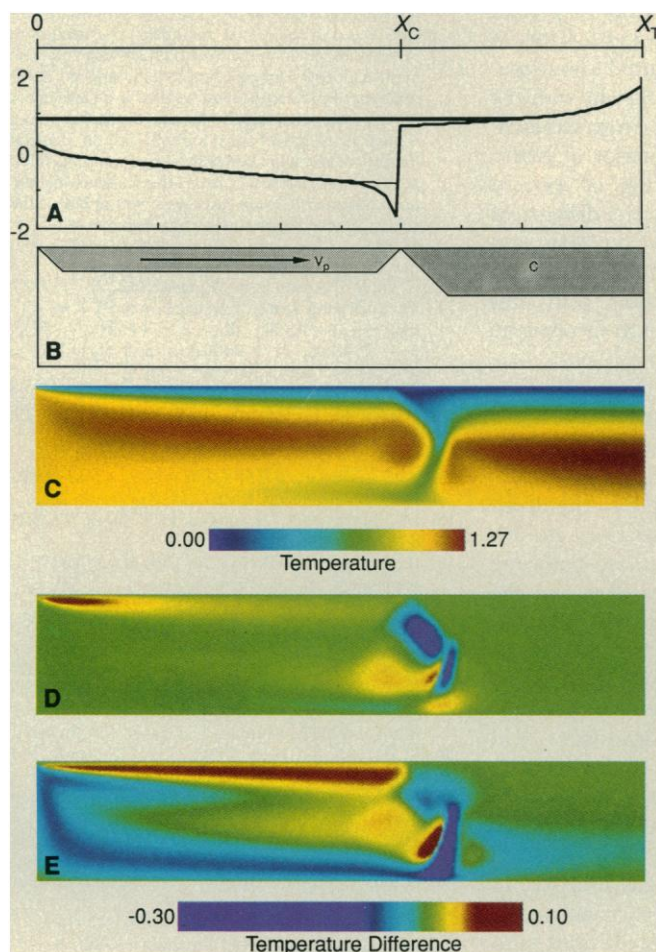


Fig. 1. (A) Total topography and sea surface elevation for the convection model (heavy lines) and for the boundary layer model (thin line) at time 0. (B) Schematic overview of model setup. (C) The thermal structure at non-dimensional time 0. The temperature scale, shown under C, has been normalized by the constant basal temperature. (D and E) Differential temperatures are shown and were obtained by subtracting the temperature at time zero (the instant at which spreading increases) from the temperature at time 0.10 (D) and time 4.00 (E). The parts of the box that increase in temperature become red while those parts that cool become blue. The differential temperature scale, shown under (E), has been normalized by the imposed temperature difference between the isothermal top and bottom boundaries.

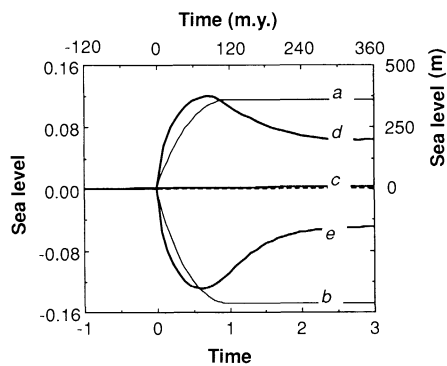


Fig. 2. Nondimensional sea level (sea level normalized by h_c) as a function of nondimensional time for the models considered. Boundary layer model shown as thin lines for a velocity that was increased by three-halves (curve *a*) and for a velocity that was decreased by two-thirds (curve *b*). Convection models shown by heavy lines for an unchanged velocity (curve *c*), a velocity increased by three-halves (curve *d*), and a velocity decreased by two-thirds (curve *e*). The scaled time shown above applies only to curves *a* and *d* and was obtained by scaling V_2 to 7.5 cm/yr and X_c to 9000 km; V_2 and X_c are defined in the text (m.y., million years).

leads to a faster subduction rate; cold fluid is rapidly dumped under the continent, and in terms of differential temperature, this process results in the cold region in Fig. 1D. As the plate continues to spread at this increased velocity, the system undergoes two changes. First, the imbalance between subduction rate and plate thickness decreases as time approaches unity and the cold (differential temperature) anomaly under the continent decreases in magnitude. Second, in the deep parts of the fluid, the temperature decrease is much larger under the ocean than under the continent; a long wavelength thermal anomaly has developed in the deep parts of the fluid, and this anomaly affects topography in an opposite sense than the shallow anomalies. This process takes 2.5 time units, the approximate time of one convective overturn. A higher rate of convective overturn leads to increased cooling of the system; on this basis, one may be led to conclude that the overall effect of increased spreading would be a decrease in sea level, but because the lithosphere is closer to the surface than the deep parts, it more strongly affects dynamic topography. Topography caused by interior density contrasts is attenuated with depth in a viscous fluid (12). Interestingly, the decrease in temperature that occurs for the deep parts of the model is approximately three times the increase associated with the lithosphere (Fig. 1E); but the final result of increased spreading is a rise in sea level.

Care must be exercised in applying the sea level curves (Fig. 2) to the earth; the transient response more likely will be a local

response to sea level changes (that is, isolated either to a single continent or to a converging plate margin), whereas the steady-state response may be applicable to global fluctuations in sea level. Moreover, in consideration of an earlier suggestion by Hager (4), if the subduction occurs in a completely oceanic environment (for example, the Tonga-Kermadec region), then instead of a transient rise in sea level following increased spreading, there may be a transient fall in sea level. Such a fall in sea level may occur because the transient differential temperature anomaly (Fig. 1D), which gives rise to a depression in dynamic topography, would occur under the oceanic lithosphere. The details of these possibilities are poorly understood, but can be investigated in more complex models.

The existence of sea level fluctuations influenced by local subduction is supported by the record of the Cretaceous transgression. Bond (13) has pointed out the correspondence between areas of Cretaceous flooding and zones of convergence, including western North America, northern Africa, and the southern part of the European platform. When North America broke away from Africa 170 million years ago, the rate of subduction off the western margin of North America would have increased; the convection models would tend to predict that continental subsidence and a jump in sea level should have occurred simultaneously. Such changes are consistent with the anomalous thickness of Cretaceous sedimentary rocks in the western interior of North America (14) and the tilting of western North America by ~ 1 km over a distance of 1400 km during the Upper Cretaceous and its subsequent rebound (15). Clearly, to make a rigorous comparison with this record, the models will have to incorporate evolving plate margins.

The calculations presented here illustrate fundamental problems with the standard lithospheric subsidence model, but also highlight exciting possibilities. Because dynamic topography is sensitive to the depth of temperature (density) variations and internal viscosity variations (16), both the temporal fluctuations in sea level and the steady-state sea level should be sensitive to internal viscosity structure. It is thus possible that the temporal and spatial record of sea level fluctuations recorded over geologic time as continental marine deposits (17) (in concert with observed plate kinematics), may place constraints on both the viscosity structure of the mantle (9) and the depth of mantle convection (18).

The usefulness of this model is limited in two respects. First, the model cannot yet be exploited to make detailed predictions as to

how sea level fluctuated over the last 120 million years; a powerful but flawed attribute of the lithospheric model is that well-constrained models of plate tectonic evolution of the oceans can be used to predict sea level. The second limitation of the convection model is that it gives no clue as to why oceanic plates undergo kinematic rearrangements. Advances now being made in modeling both spherical convection and fully dynamic plates (7, 19) should allow more realistic models to be constructed that fully exploit the geologic record of continental flooding.

REFERENCES AND NOTES

1. J. D. Hays and W. C. Pitman, *Nature* **246**, 18 (1973).
2. D. L. Turcotte and G. Schubert, *Geodynamics* (Wiley, New York, 1982).
3. M. A. Kominz, *Am. Assoc. Petrol. Geol. Mem.* **36**, 109 (1984); C. G. A. Harrison, *Eos* **70**, 1002 (1989).
4. B. H. Hager, *Eos* **61**, 374 (1980).
5. S. D. King, A. Raefsky, B. H. Hager, *Phys. Earth Planet. Inter.* **59**, 195 (1990).
6. G. F. Davies, *J. Geophys. Res.* **93**, 10451 (1988).
7. M. Gurnis and B. H. Hager, *Nature* **335**, 317 (1988); G. F. Davies, *Geophys. J.* **98**, 461 (1989).
8. The system was uniformly heated from within and had isothermal boundary conditions on the top and bottom surfaces. The realized Rayleigh number defined in terms of the total heat output (including both ocean and continent) was 4.2×10^4 . The initial velocity (in terms of a Peclet number) of the oceanic plate was 200. For the same thermal parameters but a free-slip top boundary, the maximum Peclet number along the top boundary was 262. The mesh had 160 elements horizontally and 40 vertically; the vertical refinement resulted in an average of 10 elements spanning the oceanic lithosphere. In a similar set of model runs, a mesh with an identical number of elements but with horizontal refinement at plate boundaries was used; the sea level fluctuations obtained in these cases were within 2% of the values obtained with just vertical refinement.
9. M. Gurnis, *Nature* **344**, 754 (1990); *Geophys. Res. Lett.* **17**, 623 (1990).
10. C. G. A. Harrison *et al.*, *Tectonics* **332**, 357 (1983).
11. The following values were used: $\kappa = 10^{-6} \text{ m}^2 \text{ s}^{-1}$, $(T_m - T_o) = 1300 \text{ K}$, $\alpha = 3 \times 10^{-5} \text{ K}^{-1}$, $h_c = 3140 \text{ m}$, $X_c = 9000 \text{ km}$, and $V_2 = 7.5 \text{ cm yr}^{-1}$ (for *a*) and 3.3 cm yr^{-1} (for *b*).
12. B. Parsons and S. Daly, *J. Geophys. Res.* **88**, 1129 (1983); M. A. Richards and B. H. Hager, *ibid.* **89**, 5987 (1984).
13. G. C. Bond, *Tectonophysics* **61**, 285 (1979).
14. ———, *Geology* **4**, 557 (1976); T. A. Cross and R. H. Pilger, *Nature* **274**, 653 (1978).
15. J. X. Mitrovica, C. Beaumont, G. T. Jarvis, *Tectonics* **8**, 1079 (1989).
16. B. H. Hager, *J. Geophys. Res.* **89**, 6003 (1984); J. Revenaugh and B. Parsons, *Geophys. J.* **90**, 349 (1987).
17. D. U. Wise, in *The Geology of Continental Margins*, C. A. Burke and C. L. Drake, Eds. (Springer, New York, 1974), pp. 45–58; T. D. Cook and A. W. Bally, *Stratigraphic Atlas of North and Central America* (Princeton Univ. Press, Princeton, 1975); G. C. Bond and M. A. Kominz, *J. Geophys. Res.*, in press.
18. L. Fleitout and R. N. Singh, *Terra Cognita* **8**, 143 (1988).
19. S. D. King and B. H. Hager, *Geophys. Res. Lett.*, in press.
20. Funded by National Science Foundation grants EAR-8957164 and EAR-8904660. B. Hager and H. Pollack provided helpful comments on the manuscript.

2 July 1990; accepted 12 September 1990